

**Comprehensive investigation of the Li insertion mechanism of
 $\text{Na}_2\text{Ti}_6\text{O}_{13}$ anode material for Li-ion batteries**

A. Kuhn^{†*}, J.C. Pérez-Flores[†], M. Hoelzel[‡], C. Baehtz[§], I. Sobrados[#], J. Sanz[#], F. García-Alvarado[†]

[†] Facultad de Farmacia, Departamento de Química y Bioquímica, Urbanización Montepríncipe, Universidad CEU San Pablo, 28668 Boadilla del Monte, Madrid, Spain

[‡] Forschungsneutronenquelle Heinz-Maier-Leibniz (FRM II), Technische Universität München, Lichtenbergstrasse 1, D-85747 Garching, Germany

[§] Institute of Ion Beam Physics and Materials Research, Helmholtz-Zentrum Dresden-Rossendorf, D-01314 Dresden, Germany

[#] Instituto de Ciencia de Materiales Madrid (CSIC), 28049 Cantoblanco, Madrid, Spain

SUPPORTING INFORMATION

* Corresponding author (A. Kuhn): akuhn@ceu.es

A. Kuhn et al., Figure S1

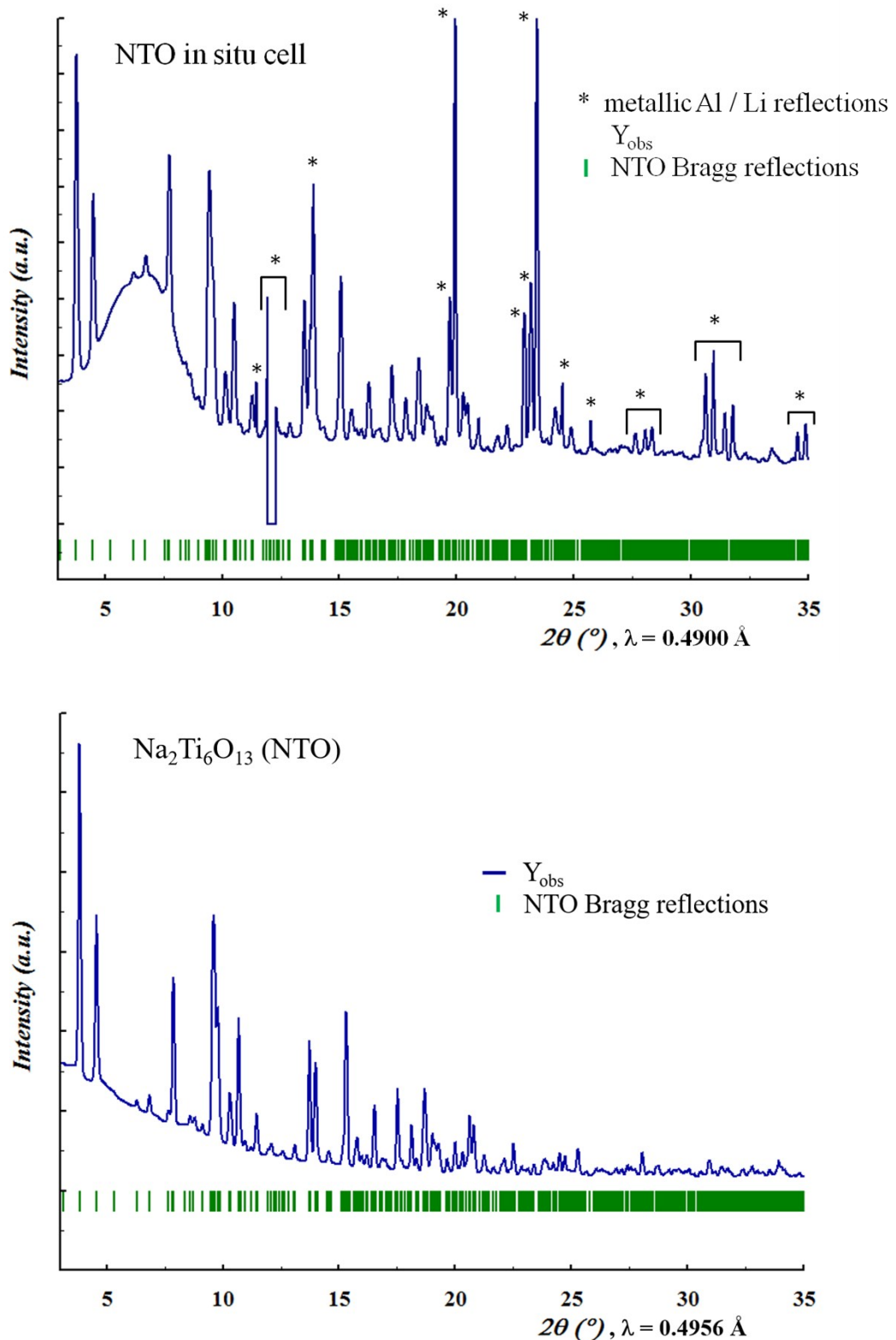


Figure S1: Synchrotron X-ray diffraction pattern of $\text{Na}_2\text{Ti}_6\text{O}_{13}$ measured in situ in the electrochemical cell (top) and ex situ (bottom) in the whole angular range. Extra Bragg reflections (from lithium and aluminum) are marked with *.

A. Kuhn et al., Figure S2

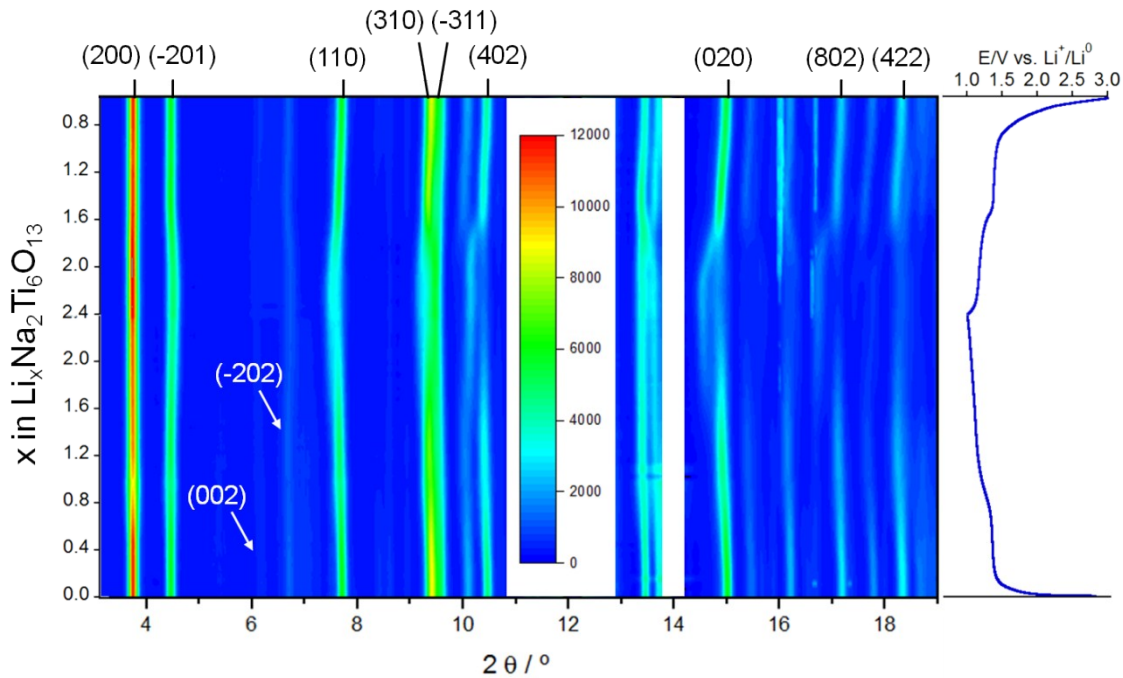


Figure S2: Synchrotron X-ray diffraction patterns collected in a $\text{Na}_2\text{Ti}_6\text{O}_{13}/\text{Li}$ in situ cell throughout the first discharge-charge cycle as a function of Li composition together with the voltage profile. Relative intensities of Bragg reflections are given by the color scale displayed in this two-dimensional contour diagram.

A. Kuhn et al., Figure S3

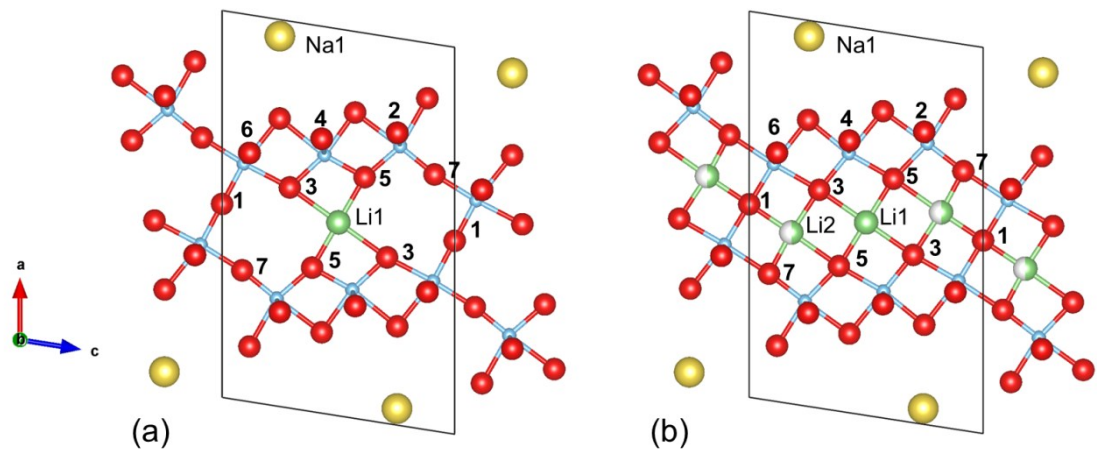


Figure S3: [010] view of the structure of $\text{Li}_{0.8}\text{Na}_2\text{Ti}_6\text{O}_{13}$ (a) and $\text{Li}_{1.7}\text{Na}_2\text{Ti}_6\text{O}_{13}$ (b), both space group C2/m. The *a*-axis is vertical to a $\text{Ti}_6\text{O}_{13}^{2-}$ layer. Only atoms at $y = \frac{1}{2}$ are shown for clarity. Na and Li atoms are labelled, O atoms are numbered and Ti atoms denoted with small circles.

A. Kuhn et al., Figure S4

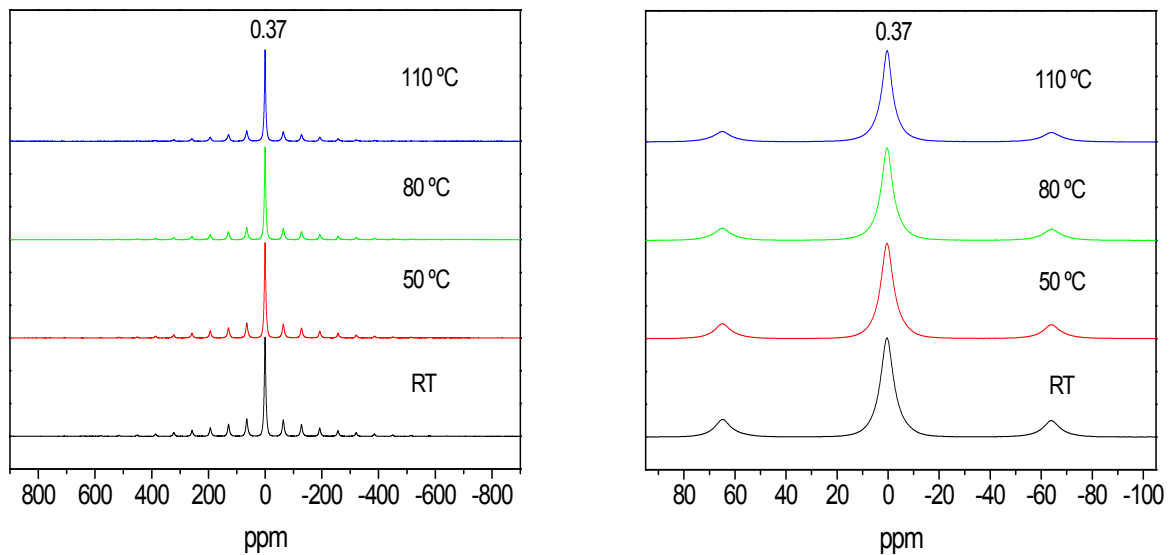


Figure S4: Thermal evolution of ⁷Li MAS-NMR spectra of Li inserted $\text{Li}_{0.8}\text{Na}_2\text{Ti}_6\text{O}_{13}$.

A. Kuhn et al., Table S1

Table S1: Comparison of structural refinements of $\text{Na}_2\text{Ti}_6\text{O}_{13}$ measured *in situ* with transmission geometry in the electrochemical cell, performed in a capillary with Debye-Scherrer geometry (both with synchrotron X-ray diffraction), and for the same compound measured with conventional X-ray diffraction and neutron diffraction.

	a / Å	b / Å	c / Å	β / °	V / Å³
Published XRD (ref. 19)	15.0949(2)	3.7452(8)	9.1693(5)	99.01	511.97
	15.1075(4)	3.74474(8)	9.1735(2)	99.031(3)	512.54(2)
	15.1032(2)	3.74373(4)	9.1713(12)	99.056(1)	512.10(1)
Refined <i>in situ</i> SXRD (this work)	15.0966(5)	3.7395(1)	9.1733(3)	99.038(2)	511.44(3)
Refined <i>ex situ</i> SXRD (this work)	15.0972(7)	3.7427(2)	9.1672(5)	99.057(3)	511.53(4)

A. Kuhn et al., Table S2**Table S2:** Selected interatomic distances (\AA) in $\text{Li}_{0.8}\text{Na}_2\text{Ti}_6\text{O}_{13}$

Na(1)-O(1) x 2	3.095(3)	Na(1)-O(3) x 2	2.525(3)	Na(1)-O(5) x 2	2.700(3)
Na(1)-O(7) x 2	2.859(3)				
Ti(1)-O(1)	1.789(6)	Ti(1)-O(2)	2.246(6)	Ti(1)-O(3)	2.026(7)
Ti(1)-O(6) x 2	1.931(2)	Ti(1)-O(7)	1.910(7)		
Ti(2)-O(2)	2.255(7)	Ti(2)-O(3)	1.852(6)	Ti(2)-O(4)	2.042(6)
Ti(2)-O(4) x 2	1.980(2)	Ti(2)-O(5)	1.787(7)		
Ti(3)-O(2) x 2	1.950(2)	Ti(3)-O(4)	2.196(7)	Ti(3)-O(5)	1.835(7)
Ti(3)-O(6)	2.151(7)	Ti(3)-O(7)	1.733(7)		
Li(1)-O(3) x 2	2.335(2)	Li(1)-O(5) x 2	2.038 (2)		

A. Kuhn et al., Table S3

Table S3: Selected distances between cations (\AA) in $\text{Li}_x\text{Na}_2\text{Ti}_6\text{O}_{13}$

Atom1-atom2	$\text{Na}_2\text{Ti}_6\text{O}_{13}$	$\text{Li}_{0.8}\text{Na}_2\text{Ti}_6\text{O}_{13}$	$\text{Li}_{1.7}\text{Na}_2\text{Ti}_6\text{O}_{13}$
Na – Ti1 (\AA)	3.520(6)	3.466(6)	3.464(6)
	3.839(7)	3.838(7)	3.850(7)
Na – Ti2 (\AA)	3.745(6)	3.743(6)	3.846(6)
	4.059(6)	4.097(6)	4.230(6)
Na – Ti3 (\AA)	3.352(7)	3.472(7)	3.394(7)
Li1 – Ti1 (\AA) ("central Li")	-	4.284(6)	4.273(6)
Li1 – Ti2 (\AA)	-	2.694(6)	2.784(6)
Li1 – Ti3 (\AA)	-	3.936(7)	3.910(7)
Li2 – Ti1 (\AA) ("lateral Li")	-	-	2.767(6)
			2.651(7)
Li2 – Ti2 (\AA)	-	-	3.825(6) 4.277(7)
Li2 – Ti3 (\AA)	-	-	2.748(7) 4.664(4)
Li3 – Ti1 (\AA) ("vault Li")	-	-	4.065(6)
Li3 – Ti2 (\AA)	-	-	2.594(4) 4.228(5)
Li3 – Ti3 (\AA)	-	-	3.885(6) 4.958(6)

A. Kuhn et al., Table S4**Table S4:** Selected interatomic distances (\AA) in $\text{Li}_{1.7}\text{Na}_2\text{Ti}_6\text{O}_{13}$

Na(1)-O(1) x 2	3.070(3)	Na(1)-O(3) x 2	2.498(4)	Na(1)-O(5) x 2	2.701(3)
Na(1)-O(7) x 2	2.902(4)				
Ti(1)-O(1)	1.833(4)	Ti(1)-O(2)	2.191(5)	Ti(1)-O(3)	2.074(5)
Ti(1)-O(6) x 2	1.932(2)	Ti(1)-O(7)	2.088(5)		
Ti(2)-O(2)	2.066(6)	Ti(2)-O(3)	1.813(5)	Ti(2)-O(4)	2.123(5)
Ti(2)-O(4) x 2	1.965(2)	Ti(2)-O(5)	1.976(6)		
Ti(3)-O(2) x 2	1.952(2)	Ti(3)-O(4)	2.148(4)	Ti(3)-O(5)	1.916(4)
Ti(3)-O(6)	2.104(4)	Ti(3)-O(7)	1.723(4)		
Li(1)-O(3) x 2	2.229(3)	Li(1)-O(5) x 2	1.996(3)		
Li(2)-O(1)	1.896(10)	Li(2)-O(3)	2.014(12)	Li(2)-O(5)	2.376(10)
Li(2)-O(7)	1.794(14)				
Li(3)-O(3) x 2	2.403(6)	Li(3)-O(5) x 2	2.358(6)	Li(3)-O(4)	1.825(15)

A. Kuhn et al., Table S5**Table S5:** Bond Valence Sum (BVS) calculated for $\text{Li}_x\text{Na}_2\text{Ti}_6\text{O}_{13}$

	$\text{Na}_2\text{Ti}_6\text{O}_{13}$	$\text{Li}_{0.8}\text{Na}_2\text{Ti}_6\text{O}_{13}$	$\text{Li}_{1.7}\text{Na}_2\text{Ti}_6\text{O}_{13}$
Na	0.654	0.632	0.645
Ti1	4.205	3.923	3.747
Ti2	4.124	3.852	3.928
Ti3	4.154	4.072	4.289
Li1	-	0.617	0.732
Li2	-	-	1.038
Li3	-	-	0.717

A. Kuhn et al., Table S6

Table S6: Li site occupancies of $\text{Li}_{1.7}\text{Na}_2\text{Ti}_6\text{O}_{13}$ deduced from neutron diffraction and ${}^7\text{Li}$ NMR spectroscopy data at 300 K.

Atom type	${}^7\text{Li}$ NMR	Neutron diffraction
Li(1)	0.817	0.82(2)
Li(2)	0.311	0.31(1)
Li(3)	0.130	0.13(1)

A. Kuhn et al., Table S7

Table S7: Chemical shift, linewidth at half height and area of each component for $\text{Li}_{1.7}\text{Na}_2\text{Ti}_6\text{O}_{13}$ deduced from ^7Li MAS NMR

	Li2	Li1	Li3			
297K	δ (ppm) width (ppm) area (%)	7.39 10.4 36.63	δ (ppm) width (ppm) area (%)	0.56 6.9 48.09	δ (ppm) width (ppm) area (%)	40.00 20.0 15.28
313K	δ (ppm) width (ppm) area (%)	7.61 9.2 35.49	δ (ppm) width (ppm) area (%)	0.29 6.5 48.70	δ (ppm) width (ppm) area (%)	37.59 20.9 15.81
333K	δ (ppm) width (ppm) area (%)	7.15 8.0 35.49	δ (ppm) width (ppm) area (%)	0.45 6.0 45.66	δ (ppm) width (ppm) area (%)	32.80 21.7 18.85
353K	δ (ppm) width (ppm) area (%)	7.15 9.3 38.17	δ (ppm) width (ppm) area (%)	0.33 5.3 45.53	δ (ppm) width (ppm) area (%)	29.52 18.3 16.29
374K	δ (ppm) width (ppm) area (%)	6.75 8.1 36.20	δ (ppm) width (ppm) area (%)	0.39 5.6 48.66	δ (ppm) width (ppm) area (%)	25.30 11.3 15.15
393K	δ (ppm) width (ppm) area (%)	6.20 7.9 37.96	δ (ppm) width (ppm) area (%)	0.30 5.7 49.18	δ (ppm) width (ppm) area (%)	22.27 8.6 12.86
413K	δ (ppm) width (ppm) area (%)	3.20 12.0 38.81	δ (ppm) width (ppm) area (%)	0.30 5.0 49.35	δ (ppm) width (ppm) area (%)	18.67 12.9 11.84
RT	δ (ppm) width (ppm) area (%)	5.23 11.0 41.60	δ (ppm) width (ppm) area (%)	0.60 6.9 52.31	δ (ppm) width (ppm) area (%)	40.63 18.3 6.09